

Article

# Preparation and Properties of Poly(imide-siloxane) Copolymer Composite Films with Micro-Al<sub>2</sub>O<sub>3</sub> Particles

Ju-Young Choi <sup>1</sup>, Kyeong-Nam Nam <sup>1</sup>, Seung-Won Jin <sup>1</sup>, Dong-Min Kim <sup>1</sup>, In-Ho Song <sup>1</sup>,  
Hyeong-Joo Park <sup>2</sup>, Sungjin Park <sup>1</sup> and Chan-Moon Chung <sup>1,2,\*</sup>

<sup>1</sup> Department of Chemistry, Yonsei University, Wonju, Gangwon-do 26493, Korea; c jy0510@yonsei.ac.kr (J.-Y.C.); nkn001@yonsei.ac.kr (K.-N.N.); jinsw0906@yonsei.ac.kr (S.-W.J.); dmkimr@yonsei.ac.kr (D.-M.K.); segunda@yonsei.ac.kr (I.-H.S.); sjpsi@yonsei.ac.kr (S.P.)

<sup>2</sup> Department of Chemistry and Medical Chemistry, Yonsei University, Wonju, Gangwon-do 26493, Korea; hyeongjoo1016@yonsei.ac.kr

\* Correspondence: cmchung@yonsei.ac.kr; Tel.: +82-033-760-2266

Received: 11 January 2019; Accepted: 1 February 2019; Published: 6 February 2019



**Abstract:** In the current study, poly(imide-siloxane) copolymers (PIs) with different siloxane contents were synthesized and used as a matrix material for PI/Al<sub>2</sub>O<sub>3</sub> composites. The PIs were characterized via their molecular weight, film quality, and thermal stability. Among the PI films, free-standing and flexible PI films were selected and used to prepare PI/Al<sub>2</sub>O<sub>3</sub> composite films, with different Al<sub>2</sub>O<sub>3</sub> loadings. The thermal conductivity, thermal stability, mechanical property, film flexibility, and morphology of the PI/Al<sub>2</sub>O<sub>3</sub> composite films were investigated for their application as heat-dissipating material.

**Keywords:** poly(imide-siloxane) copolymer; Al<sub>2</sub>O<sub>3</sub>; thermal conductivity; heat-dissipating

## 1. Introduction

Recent electronic devices such as smart applications and laptops are becoming smaller and lighter with developments in the electronics industry [1–3]. To ensure the proper operation of smaller devices, unwanted heat that is generated in electronic devices must be removed. The dissipation of heat has attracted increasing attention, and is an important issue that requires resolution [4,5]. Currently, polymer composite materials containing ceramic powder are widely used as heat dissipation materials in electronic devices [6,7].

Among the polymer materials, polysiloxane has some advantages and is used as a heat-dissipating polymer matrix [8–10]. It is composed of a linear Si-O-Si moiety with a bond-angle between 104° and 180°, which introduces flexibility to the polymer [11,12]. In addition, polysiloxane can be used permanently without any change at 150 °C, it is able to withstand 200 °C for 1000 h, and 350 °C for shorter periods of time [13,14]. However, some studies on the long-term reliability of silicone rubber suggest that commercial high-temperature silicones, which are being aged at 250 °C could suffer from severe thermal decomposition [15–17].

Polyimides have widely been used in display, vehicle, aerospace, and microelectronic industries as high-performance material owing to their good mechanical properties, excellent thermal stability, flexibility, low dielectric permittivity, and good chemical resistance [4,18–21]. Polyimides are also good candidates for use as thermal conductive composite materials that can be operated at high temperatures, due to their high thermal stability [22–27]. By introducing siloxane chain segments to the polyimide backbone structure, adhesion between the polyimide and inorganic materials can be improved, including the adhesion of the metal materials and other substrates [28–31]. Previously,

poly(imide-siloxane) copolymers (PIs) have been studied for applications in aerospace, separation, and microelectronics [32–35]. On the other hand, alumina ( $\text{Al}_2\text{O}_3$ ) fillers are used as thermally conductive material embedded in the polymer matrix [36–40]. Alumina is commercially very inexpensive and often employed to improve the dissipation of polymer materials' heat properties due to its better insulating qualities and higher thermal conductivity [40].

In this paper, we first report the preparation method and properties of PI composite films containing  $\text{Al}_2\text{O}_3$  particles, for their application as heat dissipating material. We report the preparation and properties of PIs with varying molar ratio of two diamines (an aromatic diamine and bis(3-aminopropyl)-terminated polydimethylsiloxane). Furthermore, PI/ $\text{Al}_2\text{O}_3$  composite films were prepared by adding various  $\text{Al}_2\text{O}_3$  contents into the PI matrix. Then the thermal conductivity, thermal stability, mechanical properties, film flexibility, and morphology of the composite films were investigated according to the change in  $\text{Al}_2\text{O}_3$  loadings.

## 2. Materials and Methods

### 2.1. Materials

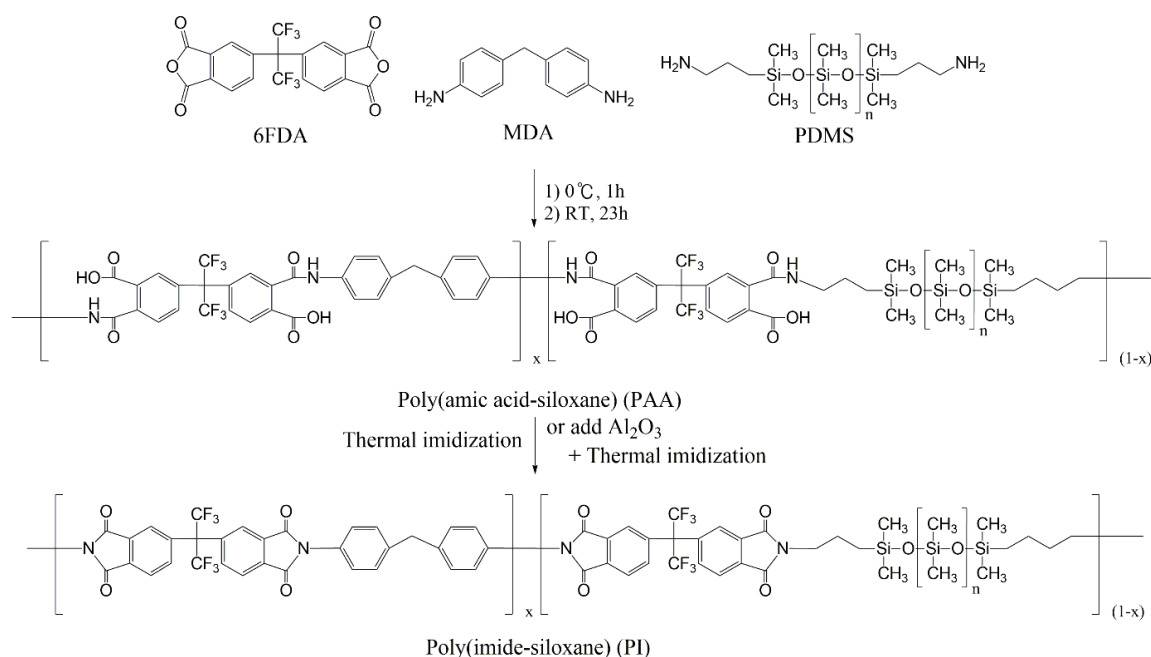
4,4'-(Hexafluoroisopropylidene) diphthalic anhydride (6FDA), 4,4'-methylenedianiline (MDA), and bis(3-aminopropyl)-terminated polydimethylsiloxane (PDMS) ( $\overline{M}_n \sim 2500$ ) were purchased from Sigma-Aldrich Korea (Seoul, Korea), and were used as received. Tetrahydrofuran (THF) was purchased from Samchun Chemicals (Seoul, Korea), distilled from  $\text{N}_2$ /benzophenone, and stored under nitrogen until use. 1-Methyl-2-pyrrolidinone (NMP) was purchased from Duksan Pure Chemical (Seoul, Korea), distilled in reduced pressure, and kept under nitrogen until use. Polyagonal alumina ( $\text{Al}_2\text{O}_3$ ; average particle size = 4  $\mu\text{m}$ ) was purchased from Denka Co. Ltd. (Seoul, Korea) and was dried at 120 °C in an oven for 24 h to remove the adsorbed water before use. Tetrahydrofuran- $d_8$  (THF- $d_8$ ) was purchased from Acros Organics BVBA (Geel, Belgium).

### 2.2. Characterization

Proton nuclear magnetic resonance ( $^1\text{H}$  NMR) spectra of samples dissolved in THF- $d_8$  were acquired using a Bruker Avance II 400 MHz spectrometer (Bruker Corporation, Billerica, MA, USA). Gel permeation chromatography (GPC; Waters Corporation, Milford, MA, USA) analysis was carried out in refractive index mode using a doubly connected Showa Denko Shodex KF-806L column at 100 °C and an eluent of 0.05 mol/L LiBr in NMP at a flow rate of 1.0 mL/min; the results were calibrated with respect to polystyrene standards. Fourier Transform Infrared (FT-IR) spectroscopy was carried out using a Spectrum One B FT-IR spectrometer (PerkinElmer, Inc., Waltham, MA, USA) using the KBr pellet technique with the following scan parameters: scan range 500–4000  $\text{cm}^{-1}$ ; number of scan 1; resolution 4  $\text{cm}^{-1}$ . Thermal analyses were carried out under a nitrogen atmosphere with a balance flow rate of 40 mL/min and a furnace flow rate of 60 mL/min using a Discovery TGA 55 (TA instrument, Inc., New Castle, DE, USA) at a heating rate of 10 °C/min. The thickness of the polyimide films was measured using a 293–348 IP65 digimatic outside micrometer (Mitutoyo Corporation, Kawasaki, Japan). Thermal conductivities (in-plane) of the composite films were measured using a LFA 467 Nanoflash (NETZSCH Korea Co., Ltd., Koyang, Korea). A universal testing machine (UTM) (QC-505M1, Daeha Trading Co., Seoul, Korea) was used to determine tensile properties. A 3-cm gauge and a strain rate of 2 cm/min were used. Film specimen measurements were performed at room temperature using 0.5 cm wide, 6 cm long, and ca. 0.3 mm thick films. An average of five individual determinations were used for each sample. Field emission scanning electron microscopy (FE-SEM) was carried out using a SU-70 (Hitachi, Ltd., Tokyo, Japan), with an acceleration voltage of 30 kV and a working distance in the range of 10 to 11.6 mm. The samples were sputter-coated with platinum.

### 2.3. Preparation of Poly(amic acid-siloxane)s (PAAs)

Scheme 1 shows the general method of copolyimide synthesis. A representative example for the synthesis of poly(amic acid-siloxane)-4 (PAA-4) (molar feed ratio of 6FDA:MDA:PDMS was 1:0.5:0.5) is described below. A dried 50-mL flask was charged with MDA (0.002 mol, 0.198 g) and PDMS (0.002 mol, 2.500 g) in THF (14.3 mL) under a nitrogen atmosphere. After 6FDA (0.004 mol, 0.888 g) was added, the resulting solution was stirred at 0 °C for 1 h, and then further stirred at room temperature for 23 h to yield a clear viscous PAA-4 solution. The other PAA solutions were prepared in a similar fashion by varying the molar feed ratio of the diamines. As an exception, NMP was used in the synthesis of PAA-1 with a molar feed ratio of 6FDA:MDA:PDMS of 1:1:0. The PAA solutions were used to prepare PI films, powders, and composite films (see below).



**Scheme 1.** Synthesis of PIs and their composites.

### 2.4. Preparation of PI Films

The PAA-4 solution obtained above was drop-cast onto slide glasses and the solution was stepwisely heated (at 50, 100, and 150 °C). The solution was allowed to stand at each temperature for 1 h. The resulting films were finally heated at 250 °C for 2 h, and PI-4 films were obtained. The PI-4 films were cooled to room temperature and put in a water bath for 1 h to allow easy peel off. The resultant films were dried in a vacuum oven at 100 °C for 1 h. The other PI films were prepared in a similar manner by varying the molar feed ratio of the diamines.

### 2.5. Preparation of PI Powders

The PAA-4 solution obtained above was poured into distilled water, forming a precipitate that was collected via filtration. The precipitate was washed with distilled water and then dried in a vacuum oven, yielding a PAA-4 powder. The PAA-4 was thermally imidized by stepwise heating in a furnace (50, 100, and 150 °C). The powder was kept for 1 h at each temperature and finally heated at 250 °C for 2 h to obtain PI-4 powder. The other PAA and PI powders were prepared in a similar manner by varying the molar feed ratio of the diamines. The prepared PAA and PI powders were used in FT-IR spectroscopy and GPC.

## 2.6. Preparation of PI Composite Films

Al<sub>2</sub>O<sub>3</sub> powder (30, 60, 75, or 80 wt%) was added to the PAA-4 solution obtained above. The mixture was ultrasonicated using an ultrasonic device (VCX750, Sonics & Materials, Newtown, CT, USA), with an output power of 150 W and a frequency of 20 kHz for 1 h to yield a milky suspension. The suspension was drop-cast onto slide glasses, and then heated in a stepwise manner (at 50, 100, and 150 °C). The suspension was allowed to stand at each temperature for 1 h and finally heated at 250 °C for 2 h to obtain PI/Al<sub>2</sub>O<sub>3</sub> composite films (PI-4-30, PI-4-60, PI-4-75, and PI-4-80). The obtained films were cooled to room temperature and put in a water bath for 1 h to facilitate peeling it off. The resultant composite films were dried in a vacuum oven at 100 °C for 1 h.

## 3. Results and Discussion

### 3.1. Preparation of PIs and Their Composite Films

The preparation of poly(imide-siloxane) copolymers (PIs) is illustrated in Scheme 1. The PIs were synthesized according to a conventional two-step procedure. During typical polyimide synthesis, aprotic polar solvents such as NMP, dimethylacetamide (DMAc), or dimethylformamide (DMF) are usually used. However, the siloxane group underwent microphase separation when aprotic solvents were used during the copolymerization. To overcome this problem, the preparation of PIs required the use of a co-solvent system or THF [41,42].

In this work, 6FDA, MDA, and PDMS were copolymerized using THF as a solvent (Table 1), except for PAA-1 which was prepared without the PDMS moiety and used NMP as a solvent. 6FDA and mixed diamines (MDA and PDMS) were first polymerized to prepare poly(amic acid-siloxane)s (PAA-1–PAA-7). The diamine molar feed ratio was controlled as summarized in Table 1. The PDMS content of PAA copolymers was determined by <sup>1</sup>H NMR (Table 1 and Figure S1). The mole percent of PDMS was calculated from the ratio of the integration values of the methyl groups in PDMS and the methylene groups of MDA. It was found that the determined values agreed well with those corresponding to PDMS contents in the feeds. The PAA solutions were drop-cast onto slide glasses and then PAAs were converted to PI-1–PI-7 films by thermal imidization. The PAA and PI powders were also prepared for characterization via FT-IR spectroscopy and GPC. Table 1 lists the molecular weights and polydispersity indexes (PDIs) of the PAAs measured by GPC. In addition, PI/Al<sub>2</sub>O<sub>3</sub> composites were prepared by adding various amount of Al<sub>2</sub>O<sub>3</sub> powder to PAA solutions. The resulting suspensions were drop-cast onto galss slides and subsequent thermal imidization was carried out to obtain PI/Al<sub>2</sub>O<sub>3</sub> composite films.

**Table 1.** Molar feed ratios and molecular weights of PAAs.

PAA Code <sup>a</sup>	Molar Feed Ratio (6FDA:MDA:PDMS)	PDMS Content (mol%) <sup>b</sup>	$\bar{M}_n$ ( $\times 10^4$ g/mol)	$\bar{M}_w$ ( $\times 10^4$ g/mol)	PDI <sup>c</sup>
PAA-1	1:1:0	-	1.03	2.32	2.2
PAA-2	1:0.9:0.1	13	10.8	37.8	3.5
PAA-3	1:0.7:0.3	32	10.8	18.1	1.6
PAA-4	1:0.5:0.5	49	3.73	13.2	3.5
PAA-5	1:0.3:0.7	70	21.1	48.8	2.3
PAA-6	1:0.1:0.9	89	16.3	50.9	3.1
PAA-7	1:0:1	-	7.92	25.1	3.2

<sup>a</sup> PAA: poly(amic acid-siloxane); <sup>b</sup> Calculated from <sup>1</sup>H NMR integrations of PAA copolymers; <sup>c</sup> Polydispersity index ( $\bar{M}_w/\bar{M}_n$ ).

### 3.2. Characterization of PAAs and PIs

The structures of PAAs and PIs were confirmed by FT-IR spectroscopy (Figure 1). FT-IR spectra of PAA-4 and PI-4 showed absorption bands at 1021 and 1095 cm<sup>-1</sup>, respectively, due to Si-O-Si stretching in the structure of PDMS. The absorption band at 1259 cm<sup>-1</sup> was also attributed to the symmetric

deformation of the  $-\text{CH}_3$  group in  $-\text{Si}(\text{CH}_3)_2-$ , and the absorption band at  $803\text{ cm}^{-1}$  was assigned to the Si-C vibration [11,41,43–45]. The FT-IR spectrum of PAA-4 showed bands at  $1721\text{ cm}^{-1}$  (carboxyl) and  $1660\text{ cm}^{-1}$  (amide) owing to C=O stretching, and at  $1545\text{ cm}^{-1}$  owing to C-N stretching (amide), suggesting the formation of PAA (Figure 1a) [11,34,46]. PI-4 exhibited absorption bands at  $1785\text{ cm}^{-1}$  owing to imide C=O asymmetric stretching,  $1726\text{ cm}^{-1}$  owing to imide C=O symmetric stretching, and  $1375\text{ cm}^{-1}$  owing to imide C-N stretching (Figure 1b) [11,34,46–48]. FT-IR spectra of the other PAAs and PIs are shown in Figures S2–S7.

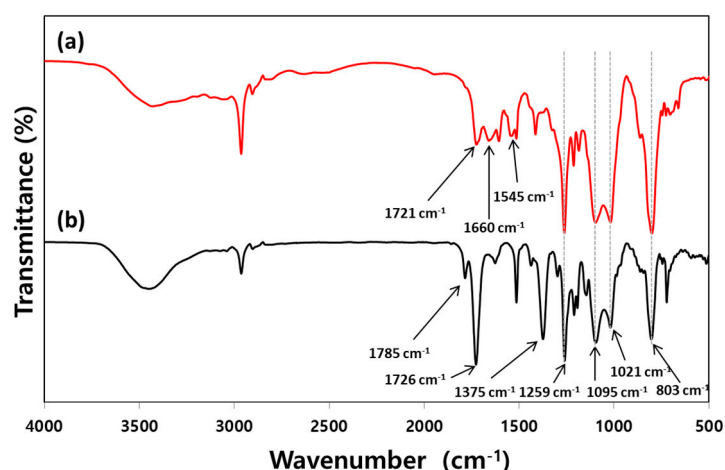


Figure 1. FT-IR spectra of (a) PAA-4, and (b) PI-4.

### 3.3. Properties of PI Films

Thermal stability of PIs was investigated by thermogravimetric analysis (TGA) (Table 2 and Figure 2). TGA was conducted to study the effects of the molar ratio of diamines on decomposition temperature ( $T_5$  and  $T_{10}$ ) and char yield of PIs.  $T_5$  and  $T_{10}$  values of the PIs ranged from 373 to 505 and 419 to 528 °C, respectively, and the decomposition temperature decreased with increasing PDMS molar ratio. Nevertheless, PIs' decomposition temperatures were much higher than those of silicone [17]. The char yield at 800 °C of PI-1 without siloxane moiety was the highest (62.4%) and the other char yields were much lower.

Table 2. Film quality and thermal properties of PIs.

PI Code <sup>a</sup>	Film Quality	$T_5$ (°C) <sup>b</sup>	$T_{10}$ (°C) <sup>c</sup>	Char Yield (%) <sup>d</sup>
PI-1	Brittle	505	528	62.4
PI-2	Brittle	446	473	28.2
PI-3	Flexible	438	454	16.7
PI-4	Flexible	428	443	0.7
PI-5	Flexible	423	441	2.1
PI-6	Sticky	403	426	4.3
PI-7	Sticky	373	419	3.2

<sup>a</sup> PI-1–PI-7 were prepared from PAA-1–PAA-7, respectively; <sup>b</sup> The temperature at which a sample exhibits 5 wt% decomposition in a nitrogen atmosphere; <sup>c</sup> The temperature at which a sample exhibits 10 wt% decomposition in a nitrogen atmosphere; <sup>d</sup> Char yield at 800 °C in a nitrogen atmosphere.

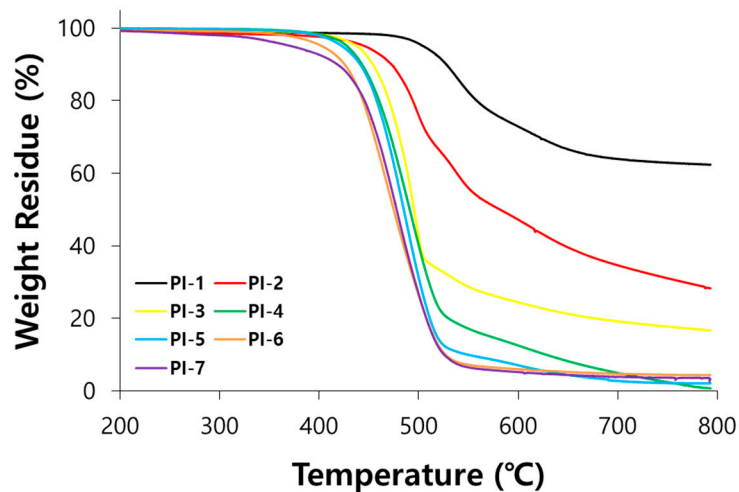


Figure 2. TGA curves of PIs.

Flexible and free-standing PI films (PI-3, PI-4, and PI-5) could be prepared from PAA-3, PAA-4, and PAA-5, respectively (Table 2 and Figure 3). When the films were bent, twisted, rolled-up, or wrapped on the 3-mm diameter bar numerous times, their appearance was almost unchanged (no damage occurred). However, PI-1 and PI-2 films were brittle due to their rigid chemical structures. On the other hand, PI-6 and PI-7 films were sticky due to the very high PDMS group contents.

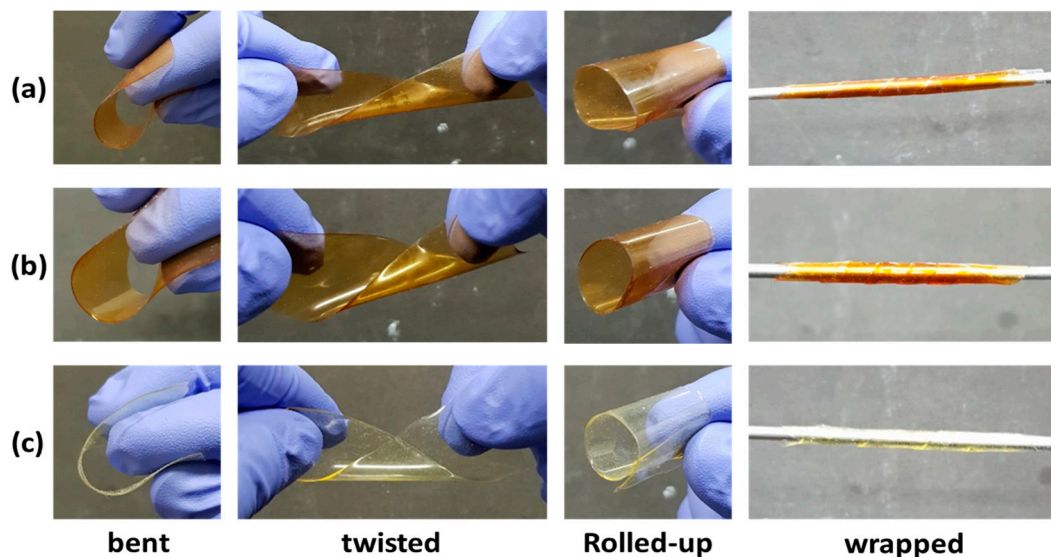
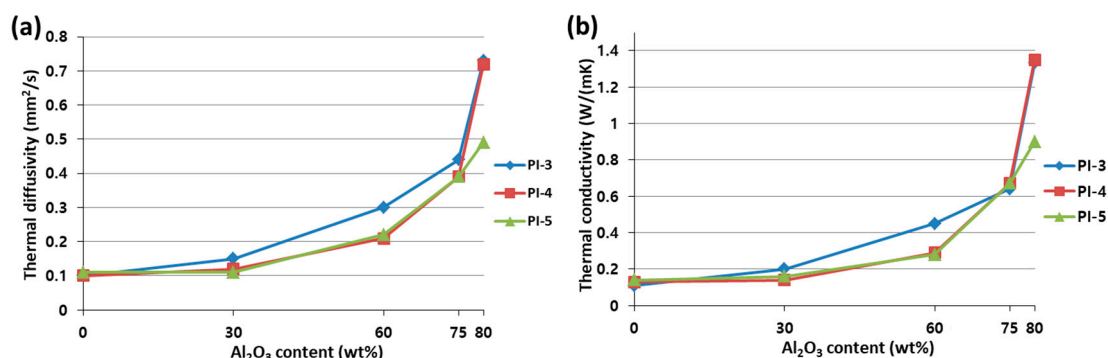


Figure 3. Photographs of (a) PI-3; (b) PI-4; (c) PI-5 films.

#### 3.4. Properties of PI/Al<sub>2</sub>O<sub>3</sub> Composite Films

Because the PI-3, PI-4, and PI-5 films were free-standing and flexible, they were used to prepare PI/Al<sub>2</sub>O<sub>3</sub> composite films. Figure 4 shows the thermal conducting properties of neat PI films and PI/Al<sub>2</sub>O<sub>3</sub> composite films, with different Al<sub>2</sub>O<sub>3</sub> loadings along an in-plane direction ( $D_{\perp}$ ) at room temperature (see Tables S1–S3). The films' thermal diffusivity ( $\alpha$ ) was determined at room temperature and under ambient pressure. From the equation  $K = \alpha \times \rho \times C_p$ , the thermal conductivity ( $K$ ) value can be calculated. In the equation,  $\rho$  is the measured film density, and  $C_p$  is the specific heat capacity of the film [5,49]. The thermal conductivities of neat PI-3, PI-4, and PI-5 were 0.11, 0.13, and 0.14 W/m·K, respectively. It is known that thermal conductivities of polyimide and polydimethylsiloxane are 0.11 and 0.25 W/m·K at room temperature, respectively [22]. The incorporation of Al<sub>2</sub>O<sub>3</sub> fillers increased thermal diffusivity and thermal conductivity of PI/Al<sub>2</sub>O<sub>3</sub> composite films (Figure 4a,b). When the

Al<sub>2</sub>O<sub>3</sub> loading was 80 wt%, PI-3 and PI-4 composites showed high thermal conductivity values, greater than 1.3 W/m·K. The thermal diffusivity and conductivity data are quite reproducible as presented in Tables S1–S3.



**Figure 4.** (a) Thermal diffusivity ( $D_{\perp}$ ), and (b) thermal conductivity ( $D_{\perp}$ ) of the PI and PI/Al<sub>2</sub>O<sub>3</sub> composite films with different Al<sub>2</sub>O<sub>3</sub> loadings.

In addition, thermal and mechanical properties of the PI/Al<sub>2</sub>O<sub>3</sub> composite films were studied (Table 3 and Figures S8 and S9). Among the flexible PI films, PI-3 was selected because it exhibited the best thermal conducting properties. The  $T_5$  and  $T_{10}$  values of the neat PI-3 and PI-3/Al<sub>2</sub>O<sub>3</sub> composite films ranged from 437 to 454 °C and 456 to 474 °C, respectively. Generally the decomposition temperatures of the PI/Al<sub>2</sub>O<sub>3</sub> composite films were higher than those of the neat PI film. The improvement in thermal stability can be attributed to restrained polymer chain mobility by Al<sub>2</sub>O<sub>3</sub> particles [17]. Furthermore, it should be noted that the PI/Al<sub>2</sub>O<sub>3</sub> composites showed much higher thermal stability compared to polysiloxane/Al<sub>2</sub>O<sub>3</sub> composites [17,50]. From the char yield data, each mass value retained around 800 °C and was almost identical to the corresponding Al<sub>2</sub>O<sub>3</sub> content in each composite.

**Table 3.** Thermal and mechanical properties of the PI-3/Al<sub>2</sub>O<sub>3</sub> composite films.

PI/Al <sub>2</sub> O <sub>3</sub> Composite Code <sup>a</sup>	$T_5$ (°C) <sup>b</sup>	$T_{10}$ (°C) <sup>c</sup>	Char Yield (%) <sup>d</sup>	Tensile Strength (MPa)	Elongation at Break (%)
PI-3	438	461	16.7	14.6 ± 2.7	210.4 ± 38.4
PI-3-30	440	456	30.7	7.3 ± 0.2	41.7 ± 2.8
PI-3-60	454	469	61.3	6.5 ± 0.4	10.4 ± 0.6
PI-3-75	450	474	75.2	5.7 ± 0.5	4.8 ± 0.6
PI-3-80	437	471	79.1	5.2 ± 0.5	3.7 ± 0.6

<sup>a</sup> PI-3, PI-3-30, PI-3-60, PI-3-75, and PI-3-80 films have Al<sub>2</sub>O<sub>3</sub> loadings of 0, 30, 60, 75, and 80 wt%, respectively; <sup>b</sup> The temperature at which a sample exhibits 5 wt% decomposition in a nitrogen atmosphere; <sup>c</sup> The temperature at which a sample exhibits 10 wt% decomposition in a nitrogen atmosphere; <sup>d</sup> Char yield at 800 °C in a nitrogen atmosphere.

The neat PI-3 film showed a tensile strength of 14.6 ± 2.7 MPa, and a high elongation at a break of 210.4 ± 38.4%. However, the PI/Al<sub>2</sub>O<sub>3</sub> composite films exhibited decreased tensile strength and elongation at break, and the mechanical properties decreased with increasing Al<sub>2</sub>O<sub>3</sub> loadings. It is well known that the incorporation of an inorganic filler to the polymer matrix reduces the polymer's flexibility. Furthermore, the polymer's strength is reduced if there are no binding sites between the polymer phase and inorganic material phase [51]. Nevertheless, the composite films with up to 75 wt% Al<sub>2</sub>O<sub>3</sub> are sufficiently flexible, as shown in Figure 5. They may be useful as a flexible heat-radiating film in flexible electronic devices requiring a high operating temperature. Even though the composite films with 80 wt% Al<sub>2</sub>O<sub>3</sub> loading are not flexible, they could also be used in high-temperature electronic devices.

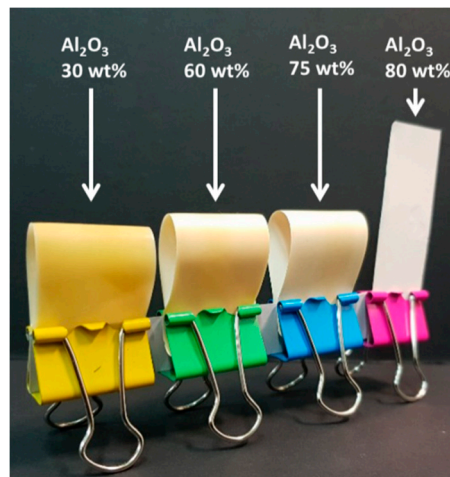


**Figure 5.** Photographs of PI composite films containing different  $\text{Al}_2\text{O}_3$  contents.

Scanning electron microscopy (SEM) was carried out to investigate the morphology of the PI/ $\text{Al}_2\text{O}_3$  composite films. Figure 6a shows the SEM image of micro- $\text{Al}_2\text{O}_3$  particles. The particles are irregularly shaped with 4  $\mu\text{m}$  average size. The neat PI-3 film before  $\text{Al}_2\text{O}_3$  addition showed a very smooth surface (Figure 6b). As shown in Figure 6c,  $\text{Al}_2\text{O}_3$  particles were well dispersed in the PI/ $\text{Al}_2\text{O}_3$  composite film and no significant fractures were observed across the film's surface.

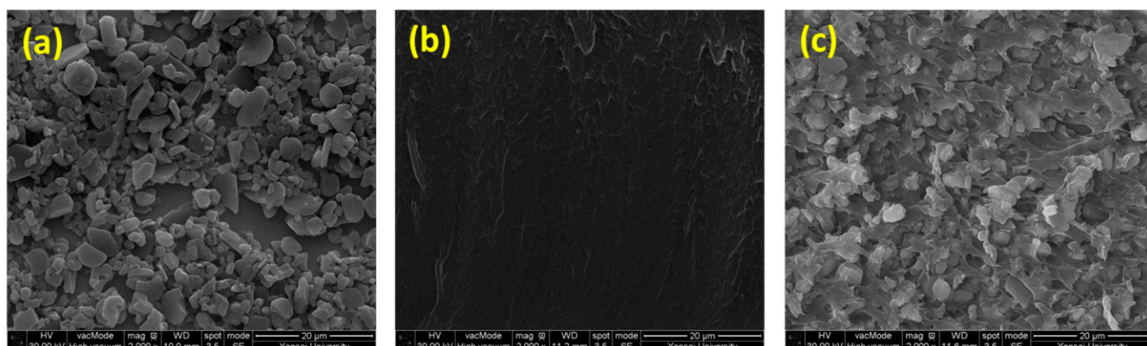


**Figure 6.** SEM images of (a)  $\text{Al}_2\text{O}_3$  particles; (b) PI-3 film; (c) PI-3-75 film.

#### 4. Conclusions

The PIs with different siloxane contents were prepared using 6FDA, MDA, and PDMS. Free-standing, flexible films of PI-3, PI-4, and PI-5 were obtained, and the PIs were used to prepare PI/ $\text{Al}_2\text{O}_3$  composite films. The thermal conductivities of the composite films increased with increasing  $\text{Al}_2\text{O}_3$  content. It was demonstrated that the composite films with up to 75 wt%  $\text{Al}_2\text{O}_3$  were both free-standing and flexible. The composite films with 80 wt%  $\text{Al}_2\text{O}_3$  loading showed a relatively good thermal conductivity, higher than 1.3 W/m·K. Besides, PI/ $\text{Al}_2\text{O}_3$  composite films exhibited higher thermal stability compared to conventional polysiloxane/ $\text{Al}_2\text{O}_3$  composites. The PI/ $\text{Al}_2\text{O}_3$  composite films could be used as a heat-radiating film in electronic devices requiring high operating temperatures.

**Supplementary Materials:** The following are available online at <http://www.mdpi.com/2076-3417/9/3/548/s1>, Figure S1: FT-IR spectra of (a) PAA-1, and (b) PI-1; Figure S2: FT-IR spectra of (a) PAA-2, and (b) PI-2; Figure S3: FT-IR spectra of (a) PAA-3, and (b) PI-3; Figure S4: FT-IR spectra of (a) PAA-5, and (b) PI-5; Figure S5: FT-IR spectra of (a) PAA-6, and (b) PI-6; Figure S6: FT-IR spectra of (a) PAA-7 and (b) PI-7; Figure S7: TGA curves of PI-3 and PI-3/ $\text{Al}_2\text{O}_3$  composite films; Figure S8: Stress–strain curves of PI-3 and PI-3/ $\text{Al}_2\text{O}_3$  composite films; Table S1: Thermal diffusivity and thermal conductivity values of the PI-3 and PI-3/ $\text{Al}_2\text{O}_3$  composite films; Table S2: Thermal diffusivity and thermal conductivity values of the PI-4 and PI-4/ $\text{Al}_2\text{O}_3$  composite films; Table S3: Thermal diffusivity and thermal conductivity values of the PI-5 and PI-5/ $\text{Al}_2\text{O}_3$  composite films.

**Author Contributions:** Conceptualization, J.-Y.C., S.P., and C.-M.C.; methodology, J.-Y.C.; formal analysis, J.-Y.C., K.-N.N., and S.-W.J.; investigation, D.-M.K., I.-H.S., and H.-J.P.; writing—original draft preparation, J.-Y.C. and C.-M.C.; writing—review and editing, C.-M.C.; supervision, C.-M.C.

**Conflicts of Interest:** The authors declare no conflict of interest.

## References

1. Gutfleisch, O.; Willard, M.A.; Bruck, E.; Chen, C.H.; Sankar, S.G.; Liu, J.P. Magnetic materials and devices for the 21st century: Stronger, lighter, and more energy efficient. *Adv. Mater.* **2011**, *23*, 821–842. [[CrossRef](#)] [[PubMed](#)]
2. Jayaprakash, N.; Das, S.K.; Archer, L.A. The rechargeable aluminum-ion battery. *Chem. Commun.* **2011**, *47*, 12610–12612. [[CrossRef](#)] [[PubMed](#)]
3. Gain, A.K.; Fouzder, T.; Chan, Y.C.; Sharif, A.; Wong, N.B.; Yung, W.K.C. The influence of addition of nano-particles on the microstructure and shear strength of eutectic Sn–Ag–Cu solder on Au/Ni metallized Cu pads. *J. Alloys Comp.* **2010**, *506*, 216–223. [[CrossRef](#)]
4. Li, T.-L.; Hsu, S.L.-C. Enhanced thermal conductivity of polyimide films via a hybrid of micro- and nano-sized boron nitride. *J. Phys. Chem. B* **2010**, *114*, 6825–6829. [[CrossRef](#)] [[PubMed](#)]
5. Wang, M.; Jiao, Z.; Chen, Y.; Hou, X.; Fu, L.; Wu, Y.; Li, S.; Jiang, N.; Yu, J. Enhanced thermal conductivity of poly(vinylidene fluoride)/boron nitride nanosheet composites at low filler content. *Compos. Part A Appl. Sci. Manuf.* **2018**, *109*, 321–329. [[CrossRef](#)]
6. Han, Z.; Fina, A. Thermal conductivity of carbon nanotubes and their polymer nanocomposites: A review. *Prog. Polym. Sci.* **2011**, *36*, 914–944. [[CrossRef](#)]
7. Huang, X.; Jiang, P.; Tanaka, T. A review of dielectric polymer composites with high thermal conductivity. *IEEE Trans. Dielectr. Electr. Insul.* **2011**, *27*, 8–16. [[CrossRef](#)]
8. Fang, H.; Zhang, X.; Zhao, Y.; Bai, S.-L. Dense graphene foam and hexagonal boron nitride filled PDMS composites with high thermal conductivity and breakdown strength. *Compos. Sci. Technol.* **2017**, *152*, 243–253. [[CrossRef](#)]
9. He, X.; Huang, Y.; Liu, Y.; Zheng, X.; Kormakov, S.; Sun, J.; Zhuang, J.; Gao, X.; Wu, D.J. Improved thermal conductivity of polydimethylsiloxane/short carbon fiber composites prepared by spatial confining forced network assembly. *J. Mater. Sci.* **2018**, *53*, 14299–14310. [[CrossRef](#)]
10. Kim, Y.; Hwang, S.; So, J.I.; Kim, C.L.; Kim, M.; Shim, S.E. Treatment of atmospheric-pressure radio frequency plasma on boron nitride for improving thermal conductivity of polydimethylsiloxane composites. *Macromol. Res.* **2018**, *26*, 864–867. [[CrossRef](#)]
11. Feng, L.; Iroh, J.O. Polyimide-b-polysiloxane copolymers: Synthesis and properties. *J. Inorg. Organomet Polym. Mater.* **2013**, *23*, 477–488. [[CrossRef](#)]
12. Barry, A.; Beck, H. *Inorganic Polymers*; Academic Press: New York, NY, USA, 1962.
13. Valentini, L.; Bittolo Bon, S.; Pugno, N.M. Severe graphene nanoplatelets aggregation as building block for the preparation of negative temperature coefficient and healable silicone rubber composites. *Compos. Sci. Technol.* **2016**, *134*, 125–131. [[CrossRef](#)]
14. Clarson, S.J. Silicones and silicone-modified materials: A concise overview. *ChemInform* **2004**, *35*, 1–10. [[CrossRef](#)]
15. Yao, Y.; Chen, Z.; Lu, G.; Boroyevich, D.; Ngo, K.D.T. Characterization of encapsulants for high-voltage high-temperature power electronic packaging. *IEEE Trans. Compon. Packag. Manuf. Technol.* **2012**, *2*, 539–547. [[CrossRef](#)]
16. Scofield, J.D.; Merrett, J.N.; Richmond, J.; Agarwal, A.; Leslie, S. Performance and Reliability Characteristics of 1200 V, 100 A, 200 °C Half-Bridge SIC MOSFET-JBS Diode Power Modules. In Proceedings of the International Conference on High Temperature Electronics, International Microelectronics & Packaging Society, Albuquerque, NM, USA, 11–13 May 2010; pp. 000289–000296.
17. Yao, Y.; Lu, G.-Q.; Boroyevich, D.; Ngo, K.D.T. Effect of Al<sub>2</sub>O<sub>3</sub> fibers on the high-temperature stability of silicone elastomer. *Polymer* **2014**, *55*, 4232–4240. [[CrossRef](#)]
18. Nakanishi, F. Photoreaction of amphiphilic diolefins in monolayers formed on an air-water interface. *J. Polym. Sci. Part C Polym. Lett.* **1988**, *26*, 159–163. [[CrossRef](#)]

19. Liaw, D.-J.; Liaw, B.-Y.; Li, L.-J.; Sillion, B.; Mercier, R.; Thiria, R.; Sekiguchi, H. Synthesis and characterization of new soluble polyimides from 3,3',4,4'-benzhydrol tetracarboxylic dianhydride and various diamines. *Chem. Mater.* **1998**, *10*, 734–739. [[CrossRef](#)]
20. Mathews, A.S.; Kim, I.; Ha, C.S. Fully aliphatic polyimides from adamantane-based diamines for enhanced thermal stability, solubility, transparency, and low dielectric constant. *J. Appl. Polym. Sci.* **2006**, *102*, 3316–3326. [[CrossRef](#)]
21. Wachsmann, E.D.; Frank, C.W. Effect of cure history on the morphology of polyimide: Fluorescence spectroscopy as a method for determining the degree of cure. *Polymer* **1988**, *29*, 1191–1197. [[CrossRef](#)]
22. Ngo, I.-L.; Jeon, S.; Byon, C. Thermal conductivity of transparent and flexible polymers containing fillers: A literature review. *Int. J. Heat Mass Transf.* **2016**, *98*, 219–226. [[CrossRef](#)]
23. Kato, R.; Maesono, A.; Tye, R.P. Thermal conductivity measurement of submicron-thick films deposited on substrates by modified ac calorimetry (laser-heating Cngstrom method). *Int. J. Thermophys.* **2001**, *22*, 617–629. [[CrossRef](#)]
24. Kurabayashi, K.; Asheghi, M.; Touzelbaev, M.; Goodson, K.E. Measurement of the thermal conductivity anisotropy in polyimide films. *J. Microelectromech. Syst.* **1999**, *8*, 180–191. [[CrossRef](#)]
25. Irwin, P.C.; Cao, Y.; Bansal, A.; Schadler, L.S. Thermal and mechanical properties of polyimide nanocomposites. In Proceedings of the 2003 IEEE Annual Report Conference on Electrical Insulation and Dielectric Phenomena, Albuquerque, NM, USA, 19–22 October 2003; pp. 120–123.
26. Guo, Y.; Xu, G.; Yang, X.; Ruan, K.; Ma, T.; Zhang, Q.; Gu, J.; Wu, Y.; Liu, H.; Guo, Z. Significantly enhanced and precisely modeled thermal conductivity in polyimide nanocomposites with chemically modified graphene via in situ polymerization and electrospinning-hot press technology. *J. Mater. Chem. C* **2018**, *6*, 3004–3015. [[CrossRef](#)]
27. Wang, T.; Wang, M.; Fu, L.; Duan, Z.; Chen, Y.; Hou, X.; Wu, Y.; Li, S.; Guo, L.; Kang, R.; et al. Enhanced thermal conductivity of polyimide composites with boron nitride nanosheets. *Sci. Rep.* **2018**, *8*, 1557. [[CrossRef](#)] [[PubMed](#)]
28. You, L. Preparation and thermal properties of silicon-containing polyimide composite films. *Chem. Eng. Trans.* **2017**, *59*, 1051–1056.
29. Lupinski, J.H.; Moore, R.S. *Polymeric Materials for Electronics Packaging and Interconnection*; American Chemical Society: Washington, DC, USA, 1989; Volume 407, p. 516.
30. Mahoney, C.M.; Gardella, J.A.; Rosenfeld, J.C. Surface characterization and adhesive properties of poly(imidesiloxane) copolymers containing multiple siloxane segment lengths. *Macromolecules* **2002**, *35*, 5256–5266. [[CrossRef](#)]
31. Homma, T.; Yamaguchi, M.; Kutsuzawa, Y.; Otsuka, N. Electrical stability of polyimide siloxane films for interlayer dielectrics in multilevel interconnections. *Thin Solid Films* **1999**, *340*, 237–241. [[CrossRef](#)]
32. Rogers, M.E.; Rodrigues, D.; Wilkes, G.L.; McGrath, J.E.; Brennan, A. Perfectly alternating segmented polyimide siloxane copolymers. In *Advances in New Materials*; Springer: Boston, MA, USA, 1992; pp. 47–55.
33. McGrath, J.E.; Dunson, D.L.; Mechem, S.J.; Hedrick, J.L. Synthesis and characterization of segmented polyimide-polyorganosiloxane copolymers. In *Progress in Polyimide Chemistry I*; Springer: Berlin/Heidelberg, Germany, 1999; pp. 61–105.
34. Zou, L.; Anthamatten, M. Synthesis and characterization of polyimide-polysiloxane segmented copolymers for fuel cell applications. *J. Polym. Sci. Part A Polym. Chem.* **2007**, *45*, 3747–3758. [[CrossRef](#)]
35. Pechar, T.W.; Kim, S.; Vaughan, B.; Marand, E.; Baranauskas, V.; Riffle, J.; Jeong, H.K.; Tsapatsis, M. Preparation and characterization of a poly(imide siloxane) and zeolite L mixed matrix membrane. *J. Memb. Sci.* **2006**, *277*, 210–218. [[CrossRef](#)]
36. Bujard, P.; Kuhnlein, G.; Ino, S.; Shiobara, T. Thermal conductivity of molding compounds for plastic packaging. *IEEE Trans. Compon. Packag. Manuf. Technol.* **1994**, *17*, 527–532. [[CrossRef](#)]
37. Droval, G.; Feller, J.-F.; Salagnac, P.; Glouannec, P. Thermal conductivity enhancement of electrically insulating syndiotactic poly(styrene) matrix for diphasic conductive polymer composites. *Polym. Adv. Technol.* **2006**, *17*, 732–745. [[CrossRef](#)]
38. Shimazaki, Y.; Hojo, F.; Takezawa, Y. Preparation and characterization of thermoconductive polymer nanocomposite with branched alumina nanofiber. *Appl. Phys. Lett.* **2008**, *92*, 133309. [[CrossRef](#)]
39. Shimazaki, Y.; Hojo, F.; Takezawa, Y. Highly thermoconductive polymer nanocomposite with a nanoporous  $\alpha$ -alumina sheet. *ACS Appl. Mater. Interfaces* **2009**, *1*, 225–227. [[CrossRef](#)]

40. Li, H.; Liu, G.; Liu, B.; Chen, W.; Chen, S. Dielectric properties of polyimide/ $\text{Al}_2\text{O}_3$  hybrids synthesized by in-situ polymerization. *Mater. Lett.* **2007**, *61*, 1507–1511. [[CrossRef](#)]
41. Ha, S.Y.; Oh, B.-K.; Lee, Y.M. Preparation of poly(amideimide siloxane) from trimellitic anhydride chloride, oxylen diamine and oligo(dimethylsiloxane) diamine. *Polymer* **1995**, *36*, 3549–3553. [[CrossRef](#)]
42. Bowns, A.D. *Synthesis and Characterization of Poly (Siloxane Imide) Block Copolymers and End-Functional Polyimides for Interphase Applications*; Virginia Tech: Blacksburg, VA, USA, 1999.
43. Deng, X.; Luo, R.; Chen, H.; Liu, B.; Feng, Y.; Sun, Y. Synthesis and surface properties of pdms–acrylate emulsion with gemini surfactant as co-emulsifier. *Colloid Polym. Sci.* **2007**, *285*, 923–930. [[CrossRef](#)]
44. Téllez, L.; Rubio, J.; Rubio, F.; Morales, E.; Oteo, J.L. FT-IR study of the hydrolysis and polymerization of tetraethyl orthosilicate and polydimethyl siloxane in the presence of tetrabutyl orthotitanate. *Spectrosc. Lett.* **2004**, *37*, 11–31. [[CrossRef](#)]
45. Li, K.; Zeng, X.; Li, H.; Lai, X.; Xie, H. Effects of calcination temperature on the microstructure and wetting behavior of superhydrophobic polydimethylsiloxane/silica coating. *Colloids Surf. A Physicochem. Eng. Asp.* **2014**, *445*, 111–118. [[CrossRef](#)]
46. Zhang, K.; Yu, Q.; Zhu, L.; Liu, S.; Chi, Z.; Chen, X.; Zhang, Y.; Xu, J. The Preparations and Water Vapor Barrier Properties of Polyimide Films Containing Amide Moieties. *Polymers* **2017**, *9*, 677. [[CrossRef](#)]
47. Yu, H.-C.; Choi, J.-Y.; Jeong, J.-W.; Kim, B.-J.; Chung, C.-M. Simple and easy recycling of poly(Amic Acid) gels through microwave irradiation. *J. Polym. Sci. Part A Polym. Chem.* **2017**, *55*, 981–987. [[CrossRef](#)]
48. Choi, J.-Y.; Yu, H.-C.; Lee, J.; Jeon, J.; Im, J.; Jang, J.; Jin, S.-W.; Kim, K.-K.; Cho, S.; Chung, C.-M. Preparation of polyimide/graphene oxide nanocomposite and its application to nonvolatile resistive memory device. *Polymers* **2018**, *10*, 901. [[CrossRef](#)]
49. Muratov, D.S.; Kuznetsov, D.V.; Il'inykh, I.A.; Burmistrov, I.N.; Mazov, I.N. Thermal conductivity of polypropylene composites filled with silane-modified hexagonal BN. *Compos. Sci. Technol.* **2015**, *111*, 40–43. [[CrossRef](#)]
50. Cinausero, N.; Azema, N.; Cochez, M.; Ferriol, M.; Essahli, M.; Ganachaud, F.; Lopez-Cuesta, J.M. Influence of the surface modification of alumina nanoparticles on the thermal stability and fire reaction of PMMA composites. *Polym. Adv. Technol.* **2008**, *19*, 701–709. [[CrossRef](#)]
51. Chen, Y.; Iroh, J.O. Synthesis and characterization of polyimide/silica hybrid composites. *Chem. Mater.* **1999**, *11*, 1218–1222. [[CrossRef](#)]



© 2019 by the authors. Licensee MDPI, Basel, Switzerland. This article is an open access article distributed under the terms and conditions of the Creative Commons Attribution (CC BY) license (<http://creativecommons.org/licenses/by/4.0/>).